Two-Dimensional Modelling
of the ZEPHYR Experiment

S.C. Jardin, D.B. Albert, W. Schneider

IPP 1/184 February 1981

MAX-PLANCK-INSTITUT FÜR PLASMAPHYSIK

8046 GARCHING BEI MÜNCHEN

MAX-PLANCK-INSTITUT FÜR PLASMAPHYSIK

GARCHING BEI MÜNCHEN

Two-Dimensional Modelling of the ZEPHYR Experiment

S.C. Jardin, D.B. Albert, W. Schneider

IPP 1/184 February 1981

Die nachstehende Arbeit wurde im Rahmen des Vertrages zwischen dem Max-Planck-Institut für Plasmaphysik und der Europäischen Atomgemeinschaft über die Zusammenarbeit auf dem Gebiete der Plasmaphysik durchgeführt.

IPP 1/184

S.C. Jardin
D.B. Albert
W. Schneider

Two Dimensional Modelling of the ZEPHYR Experiment

September 1980 (in English)

Abstract

A two-dimensional transport code, based on a description due to Hirshman and Jardin, has been used to model a typical discharge for the ZEPHYR experiment. We describe here the equations solved by this code and present the results of this calculation.

The reduced set of transport equations, derived in Ref. /1/, can be summarized as follows:

$$(N_j')_t + (N_j' u)_\psi = -(V'\Gamma_j)_\psi + V'\langle S_{n_j}\rangle \tag{1a}$$

$$(\sigma')_t + (\sigma' u)_\psi = -\frac{2}{5}\left(\frac{\sigma'}{p}\right) S \tag{1b}$$

$$(\sigma_e')_t + (\sigma_e' u)_\psi = -\frac{2}{5}\left(\frac{\sigma_e'}{p_e}\right) S_e \tag{1c}$$

$$(\chi')_t + (\chi' u)_\psi = (2\pi E_\parallel^*)_\psi \tag{1d}$$

$$(\Psi')_t + (\Psi' u)_\psi = 0 \tag{1e}$$

$$\left\{(16\pi^3 \chi^2)^{-1}\chi'\Delta^* + \mathcal{L}_0 + \mathcal{L}_1\right\}\Omega \tag{2}$$
$$= 2\,\underset{\sim}{J}\cdot\underset{\sim}{\nabla}\phi\,(E_\parallel^*)_\psi + \frac{1}{2} B_p^2\left[(E_\parallel^*)_\psi/\chi'\right]_\psi - \frac{2}{3} S_\psi$$

$$x_t = \psi^{-\ell}(\xi_\theta x_\psi - \xi_\psi x_\theta) \tag{3a}$$

$$z_t = \psi^{-\ell}(\xi_\theta z_\psi - \xi_\psi z_\theta) \tag{3b}$$

Here the surface averaged entropy and electron entropy source terms are defined as

$$S \equiv -\langle J\cdot\nabla\phi\rangle E_\parallel^* + \frac{1}{V'}\sum_{j=i,e}[Q_j]_\psi - \langle S_p\rangle \tag{4a}$$

$$S_e \equiv \langle J\cdot\nabla\phi\rangle E_{\parallel}^{*} + \frac{1}{V'}[Q_e]_{\psi} + (p_i)_{\psi}\Gamma_i/n_i$$

$$+ \langle \underset{\sim}{u}_i\cdot\nabla\cdot\underset{\approx}{\pi}_i\rangle - Q_{\Delta e} - \langle S_{pe}\rangle \tag{4b}$$

and the surface averaged cross field heat flux term for species j is

$$Q_j \equiv V' \left[\langle \underset{\sim}{q}_j\cdot\underset{\sim}{\nabla}\psi\rangle + \frac{5}{2}\Gamma_j^{*}\right] \tag{5}$$

The flux coordinates (ψ , Θ) are the independent variables, along with the time t. Using any of these as a subscript denotes differentiation with the other two held fixed. The coordinates (x, ϕ , z) form a cylindrical coordinate system with ϕ being the symmetry angle. Both x and z are considered to be functions of ψ , Θ and t. The Jacobian of the transformation (x, ϕ ,z) to (ψ , Θ , ϕ) is defined as $\mathcal{J} = [\underset{\sim}{\nabla}\psi \times \underset{\sim}{\nabla}\Theta\cdot\underset{\sim}{\nabla}\phi]^{-1}$. It is taken to be of the form

$$\mathcal{J} = T\, x^{m}\psi^{\ell} \tag{6}$$

where T is a normalization constant and m and ℓ are integers. (Note that the symbol is replacing the symbol n used in Ref. /1/). If the Jacobian is initially of the form (6) and if x and z are advanced using eq. (3), then $\mathcal{J}$ will always have the form of eq. (6).

Angular brackets denote the flux surface average operator,

$$\langle a\rangle \equiv \int_0^{2\pi} d\Theta\, \mathcal{J}\, a \Big/ \int_0^{2\pi} d\Theta\, \mathcal{J} \tag{7}$$

and the differential volume is defined as

$$V' \equiv \partial\left(\int_0^{\psi} d\underset{\sim}{X}\right)/\partial\psi = 2\pi\int_0^{2\pi} \mathcal{J}\, d\Theta \tag{8}$$

The variables advanced in time in eqs. (1a) - (1e) are the differential particle number for each species

$N_j'(\psi,t) \equiv n_j(\psi,t)\,V'$, the differential plasma entropy

$\sigma'(\psi,t) \equiv [p(\psi,t)]^{3/5}\,V'$, the differential electron entropy

$\sigma_e'(\psi,t) \equiv [p_e(\psi,t)]^{3/5}\,V'$, the poloidal flux density

$\chi'(\psi,t) \equiv (2\pi)^{-1}\partial(\int_0^\psi d\underset{\sim}{X}\,\underset{\sim}{B}\cdot\nabla\theta)/\partial\psi = 2\pi\,\mathcal{J}\,\underset{\sim}{B}\cdot\nabla\theta$ and the toroidal flux density $\Psi'(\psi,t) \equiv (2\pi)^{-1}\partial(\int_0^\psi d\underset{\sim}{X}\,\underset{\sim}{B}\cdot\nabla\phi)/\partial\psi = (2\pi)^{-1} g\langle X^{-2}\rangle V'$

Here n_j is the particle density of species j, P_j is the pressure of species j, $p = p_e + p_i$, and the magnetic field is $B = B_p + B_T$, with $\underset{\sim}{B}_p = (2\pi)^{-1}\chi'(\psi,t)\,\nabla\phi\times\nabla\psi$ and $\underset{\sim}{B}_T = g(\psi,t)\nabla\phi$

The operators Δ^*, $\mathcal{L}_o$ and $\mathcal{L}_1$ are defined by

$$\Delta^* F \equiv X^2\mathcal{J}^{-1}\left[(h^{\psi\psi}F_\psi + h^{\psi\theta}F_\theta)_\psi + (h^{\psi\theta}F_\psi + h^{\theta\theta}F_\theta)_\theta\right] \tag{9}$$

where the $h^{\alpha\beta} \equiv X^{-2}\mathcal{J}\,\underset{\sim}{\nabla}\alpha\times\underset{\sim}{\nabla}\beta$ can be expressed as derivatives of the cylindrical coordinates as $h^{\psi\psi} = \mathcal{J}^{-1}(X_\theta^2 + Z_\theta^2)$, $h^{\theta\theta} = \mathcal{J}^{-1}(X_\psi^2 + Z_\psi^2)$, $h^{\psi\theta} = -\mathcal{J}^{-1}(X_\theta X_\psi + Z_\theta Z_\psi)$

$$\mathcal{L}_o(a) = (4\pi X^2)^{-1}\left\{g^2(V'\langle X^{-2}\rangle)^{-1}\left[(V'/\chi')\ \langle X^{-2}a\rangle\right]_\psi\right\}_\psi \tag{10}$$

$$\mathcal{L}_1(a) = \left[(p_\psi/\chi')_\psi + (4\pi X^2)^{-1}(gg_\psi/\chi')_\psi\right]a + \frac{5}{3}\left\{(p/V')\left[(V'/\chi')\langle a\rangle\right]_\psi\right\}_\psi \tag{11}$$

Note that $\underset{\sim}{J}\cdot\underset{\sim}{\nabla}\phi = (8\pi\mathcal{J})^{-1}\left[(h^{\psi\psi}\chi_\psi)_\psi + (h^{\psi\theta}\chi_\psi)_\theta\right]$

$$= -2\pi\left[(4\pi X^2)^{-1}gg_\psi + p_\psi\right](\chi)^{-1} \tag{12a}$$

(12b)

where the second form is obtained using the force balance equation.

We have used the symbol Ω , eq. (2), to denote (χ'/Ψ') times the absolute time derivative of the toroidal flux function, or equivalently, χ' times the normal component of the toroidal flux velocity. Thus

$$\Omega \equiv q^{-1}\left(\frac{d}{dt}\Psi\right)\Big|_{\chi} = \chi' \underset{\sim}{u}_{\Psi} \cdot \underset{\sim}{\nabla}\psi$$

where $q \equiv \Psi'/\chi'$ is the tokamak safety factor. As derived in Ref. /1/, the relative velocity of Ψ and χ' surfaces, $u(\psi,t)$, and the derivative of the coordinate stream function, $\xi_\Theta(\psi,\Theta,t)$ and $\xi_\psi(\psi,\Theta,t)$ are obtainable from Ω of eq. (2) by the relations

$$u(\psi,t) = \langle X^{-m}\Omega\rangle / (\langle X^{-m}\rangle \chi') \tag{13a}$$

$$\xi_\Theta(\psi,\Theta,t) = (\Omega - \langle X^{-m}\Omega\rangle / \langle X^{-m}\rangle)(\psi^{\ell}/\chi') \tag{13b}$$

$$\xi_\psi(\psi,\Theta,t) = \frac{\partial}{\partial\psi}\int_0^\Theta \xi_\Theta \, d\Theta \tag{13c}$$

Once the transport quantities $E_{\parallel}^{*}$, Γ_j^{*}, Q_j and $\langle \underset{\sim}{u}_j \cdot \underset{\sim}{\nabla} \cdot \underset{\approx}{\Pi}_j \rangle$ are given in terms of the plasma variables and their derivatives, the system of eqs. (1) through (3) together with the definitions in eqs . (4) through (12) provide a closed system, needing only the source functions $\langle S_{nj}\rangle$, $\langle S_p\rangle$, $\langle S_e\rangle$ and the boundary conditions to completely specify a problem. The numerical method used to solve eqs. (1) through (3) is outlined here and detailed in the next two sections.

The numerical solution procedure described here has been utilized to predict the performance of the proposed ZEPHYR experiment. In the operating scenario for this device, a deuterium-tritium tokamak plasma will be heated to near ignition conditions by intense neutral particle injection, and will then be subjected to major radius compression causing the plasma to ignite.

In add ition to neoclassical transport we have included empirical anomalous electron thermal conduction and particle transport so that $\langle \underset{\sim}{q}^e \cdot \underset{\sim}{\nabla}\psi \rangle_{anom} = -C_e \langle |\nabla\psi|^2 \rangle (T_e)_\psi$ and $\Gamma_{anom} = -(C_p/n_e)\langle |\nabla\psi|^2 \rangle (n_e)_\psi$ with the constants C_e and C_p equal to 6.25×10^{17} and 1.25×10^{17} in cgs units.

Bremsstrahlung radiation is included as a loss term for the electrons. A diffusion-like neutral gas refueling model has been used to provide a source term in the density equation with the normalization constant chosen to keep the total plasma mass constant during the entire discharge. Previous comparisons with a more involved Monte-Carlo calculation have shown this to be a reasonable approximation.

A thermonuclear fusion source term has been added to the energy equation to account for heating of the plasma by the 3.5 meV alpha particles produced by D-T fusion. If we assume the alpha-particles to give up their energy near where they are produced, this can be represented by a local source term (cgs units)

$$S_{p\alpha} = 5.047 \times 10^{-21} n_D n_T \exp\left[-0.476 \left| \ln\left(\frac{T_i}{69}\right) \right|^{2.25} \right]$$

where n_D and n_T are the deuterium and tritium density (assumed equal) and T_i is the local ion temperature in keV. This source is split 40 % to the ions and 60 % to the electrons.

Another source term is added during the time interval when the neutral beam injection is occuring, to model the plasma heating due to the slowing down of the fast injection particles, and to the alpha-particles produced by fusion events induced by these high energy injected particles. A source term in good agreement with that obtained from Monte Carlo calculations is given by

$$S_{pB} = P \left[(\psi/\psi_\ell)^2 + (d/\psi_\ell)^2 \right]^{-1} (d/\psi_\ell)^2 \left[1 - (\psi/\psi_\ell)^2 \right]$$

where $0 < \psi < \psi_\ell$ and $(d/\psi_\ell) = 0.9$. The normalization constant P is chosen so that the total power deposited is $\int_0^{\psi_\ell} V' S_{pB}(\psi)\, d\psi = 14$ MW during the injection .

Using these source and transport models, the calculation proceeds as follows. An initial plasma equilibrium is computed with R = 200 cm, a = 60 cm, toroidal magnetic field at axis $B_T = 61$ kGauss, and with plasma current $I_p = 2.47$ MA . The calculation proceeds for 0.5 sec with no external heating source, at which time the neutral beam source term is turned on and left on until $t = 1.6$ sec. The major radius compression takes place in the interval $1.5 \text{ sec} < t < 1.6$ sec, and the calculation is halted at $t = 2.0$ sec.

The boundary conditions used in this calculation are as follows. The values of n, T_e, T_i and χ' were held at fixed values at the plasma-vacuum boundary (pedestal boundary conditions) so that $n_b = 2 \times 10^{13} \text{ cm}^{-3}$, $T_{ib} = T_{eb} = 30$ eV, $q_b = 2.68$. The toroidal field in the vacuum is $\underset{\sim}{B}_T = g_V \underset{\sim}{\nabla}\phi$, with g_V a constant which gives the value $B_T = 61$ kG at $X = 200$ cm. The surface averaged part of the toroidal flux velocity at the boundary, U_b, is determined self consistently so that the equilibrium equation remains satisfied across the plasma-vacuum boundary. The surface varying part of the toroidal flux velocity is prescribed to be zero except during the compression phase at which time it is given a value corresponding to a uniform radially inward velocity.

The results of this calculation are illustrated in Figs. 1 through 4. Figure 1 shows the magnetic surfaces at time $t = 0$ (before compression) and at $t = 2$ sec (after compression). During the compression the position of the magnetic axis has decreased from $R = 207$ cm to $R = 140$ cm and the minor radius has decreased from $a = 61$ cm to $a = 48$ cm. Figure 2 shows the midplane values of p, J, n, T_e, T_i, and q at various times during the calculation, and Fig. 3 shows the central values of the temperatures and density, and the plasma β as a function of the time t.

Fig. 4 presents a graph of the stability history of this calculation to localized ballooning modes. This is obtained by evaluating the ballooning criteria on each magnetic surface almost continuously during the calculation. The physical consequences of a portion of the plasma being unstable to the linear ballooning criteria is not known at this time, however, it is of interest to note that this experiment should theoretically exceed the ballooning mode limit.

References:

/1/ Hirshmann, S.P., Jardin, S.C., Physics of Fluids 22 (1979) 731

Figure Captions

Figure 1 Constant (ψ , θ) Co-ordinate Surfaces at (a) $t = 0$ (before compression) and (b) $t = 2$ secs (after compression).

Figure 2 Profiles of the midplane values of (a) p, (b) J, (c) n, (d) T_e, (e) T_i and (f) n at various times during the discharge.

Figure 3 Time histories of the central electron (a) and ion (b) temperatures, the central density (c) and the total plasma β (d).

Figure 4 Stability history showing which magnetic surfaces are predicted to be balloon unstable at which times.

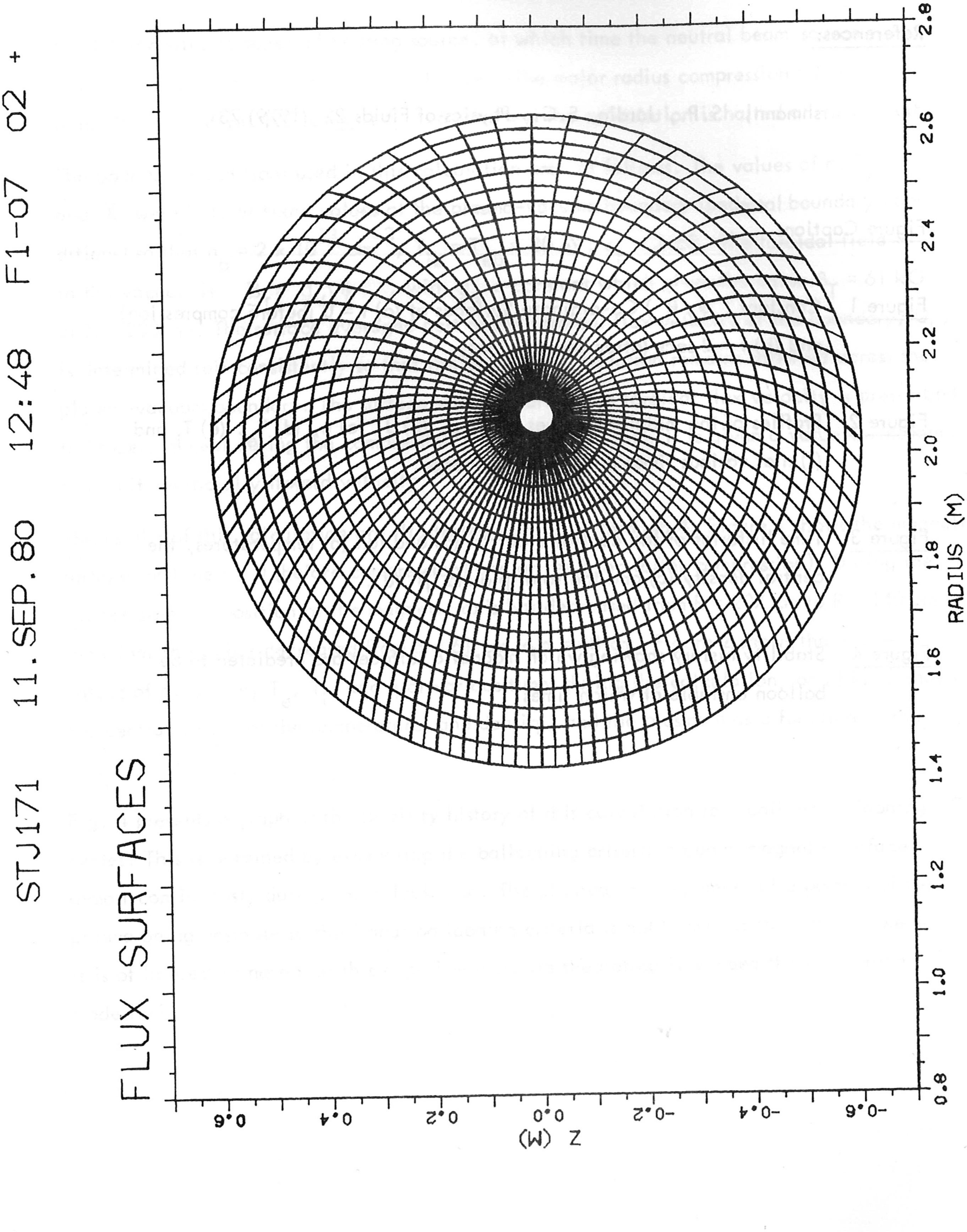
STJ171 11.SEP.80 12:48 F1-07 02 +
FLUX SURFACES
RADIUS (M)
Z (M)
0.8
1.0
1.2
1.4
1.6
1.8
2.0
2.2
2.4
2.6
2.8
0.6
0.4
0.2
0.0
-0.2
-0.4
-0.6

Figure 1a

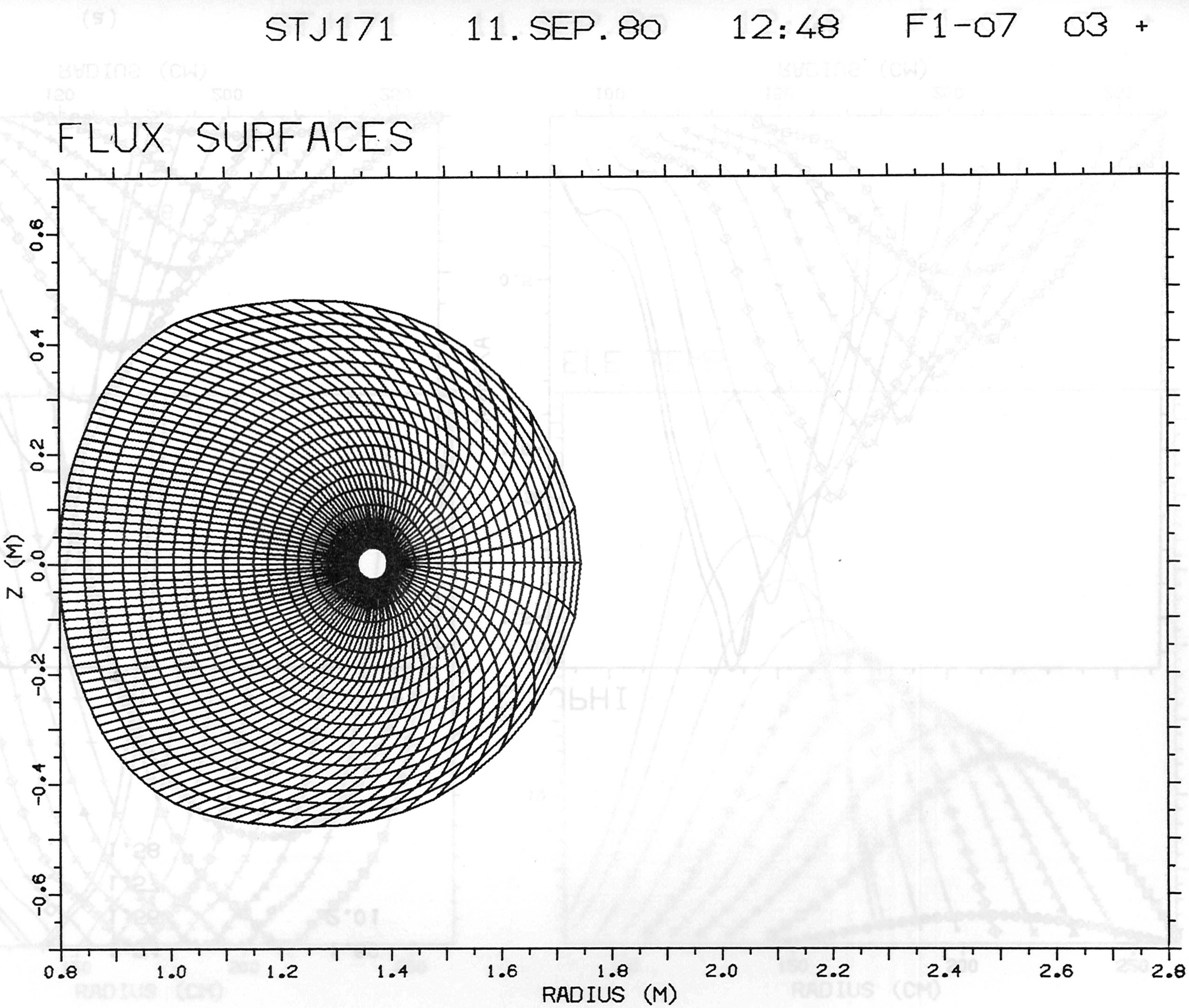
STJ171 11.SEP.80 12:48 F1-07 03 +
FLUX SURFACES
Z (M)
0.6
0.4
0.2
0.0
-0.2
-0.4
-0.6
0.8
1.0
1.2
1.4
1.6
1.8
2.0
2.2
2.4
2.6
2.8
RADIUS (M)

Figure 1b

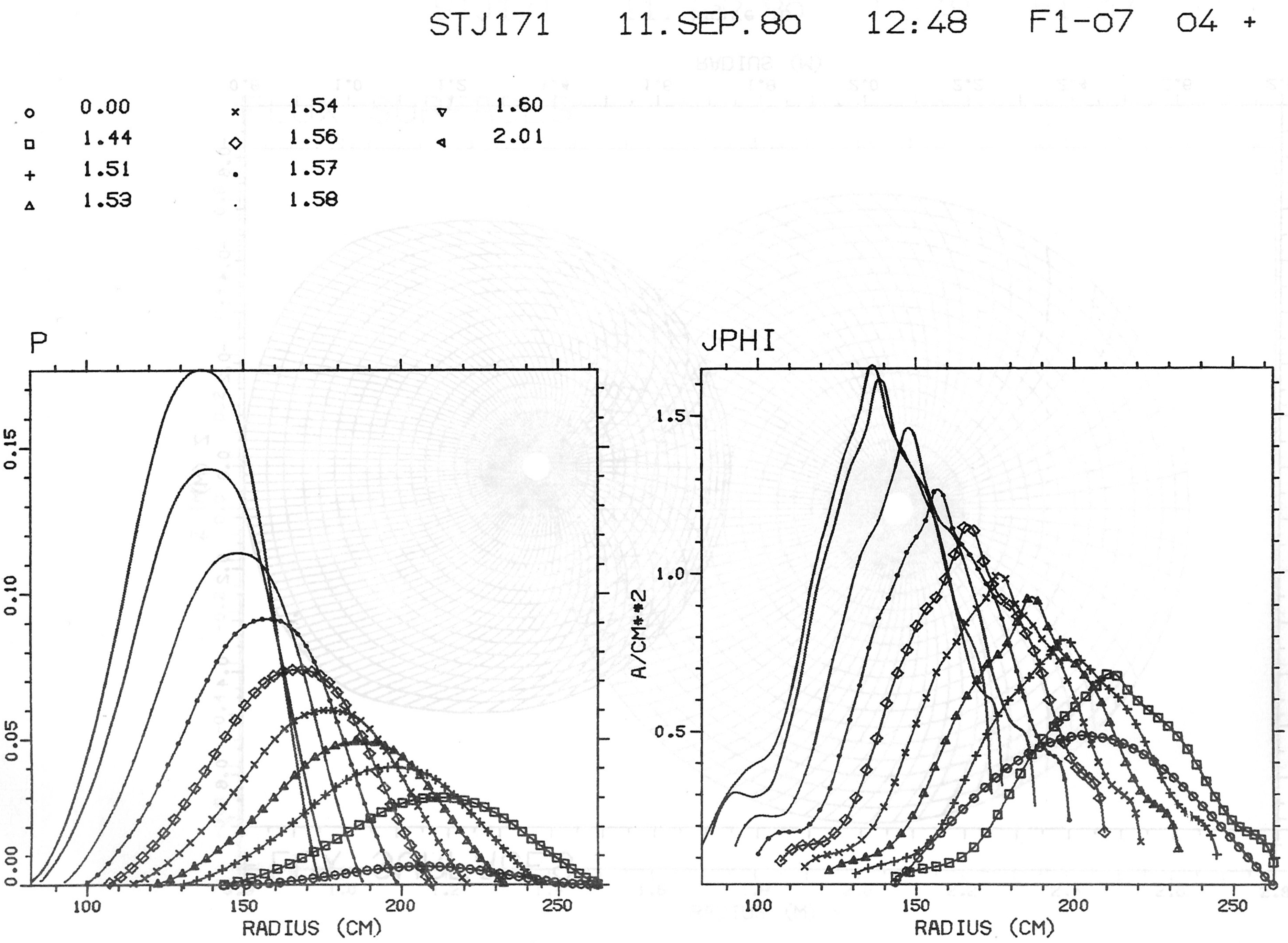

STJ171 11.SEP.80 12:48 F1-07 04 +
○ 0.00
□ 1.44
+ 1.51
△ 1.53
× 1.54
◇ 1.56
• 1.57
. 1.58
▽ 1.60
◁ 2.01
P
0.00
0.05
0.10
0.15
100
150
200
250
RADIUS (CM)
JPHI
A/CM**2
0.5
1.0
1.5
100
150
200
250
RADIUS (CM)

Figure 2 (a) (b)

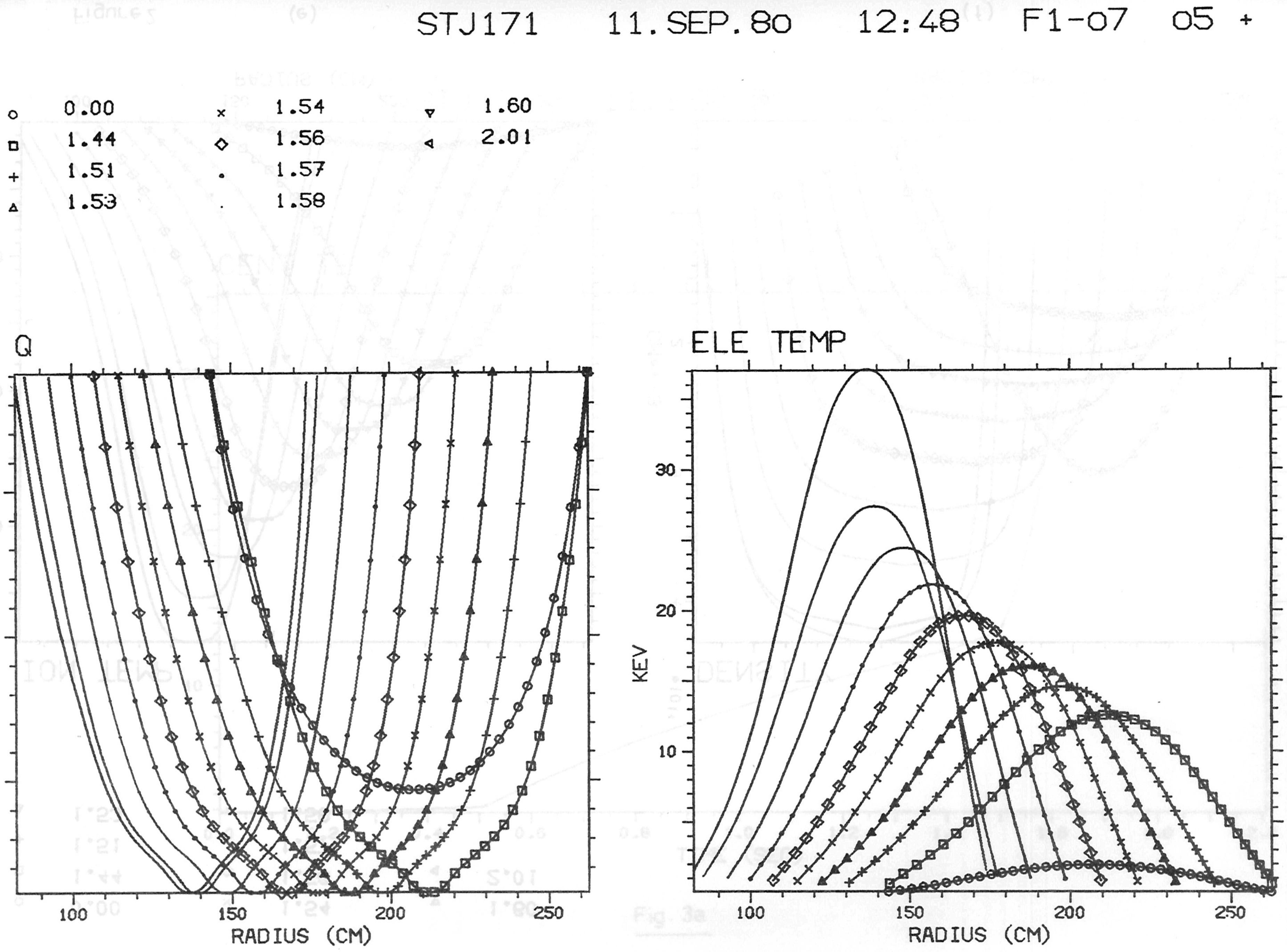
STJ171 11.SEP.80 12:48 F1-07 05 +
○ 0.00
□ 1.44
+ 1.51
△ 1.53
× 1.54
◇ 1.56
• 1.57
. 1.58
▽ 1.60
◁ 2.01
Q
2.0
1.5
1.0
100
150
200
250
RADIUS (CM)
ELE TEMP
KEV
30
20
10
100
150
200
250
RADIUS (CM)

Figure 2 (c) (d)

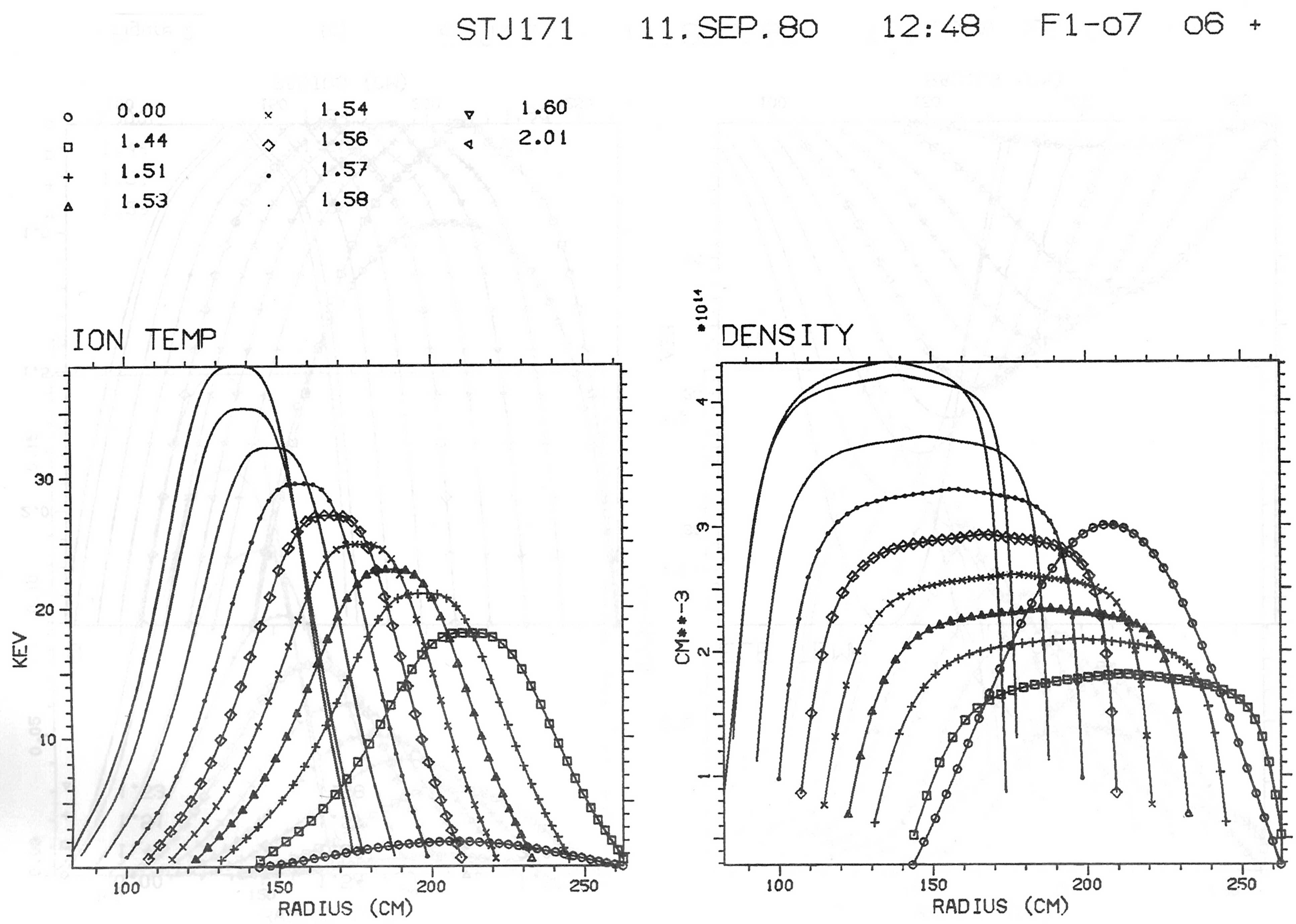
STJ171 11.SEP.80 12:48 F1-07 06 +
○ 0.00
□ 1.44
+ 1.51
△ 1.53
× 1.54
◇ 1.56
• 1.57
. 1.58
▽ 1.60
◁ 2.01
ION TEMP
KEV
30
20
10
100
150
200
250
RADIUS (CM)
DENSITY
*10^14
CM**-3
4
3
2
1
100
150
200
250
RADIUS (CM)

Figure 2 (e) (f)

STJ171 11.SEP.8o 12:48 F1-o7 11 +

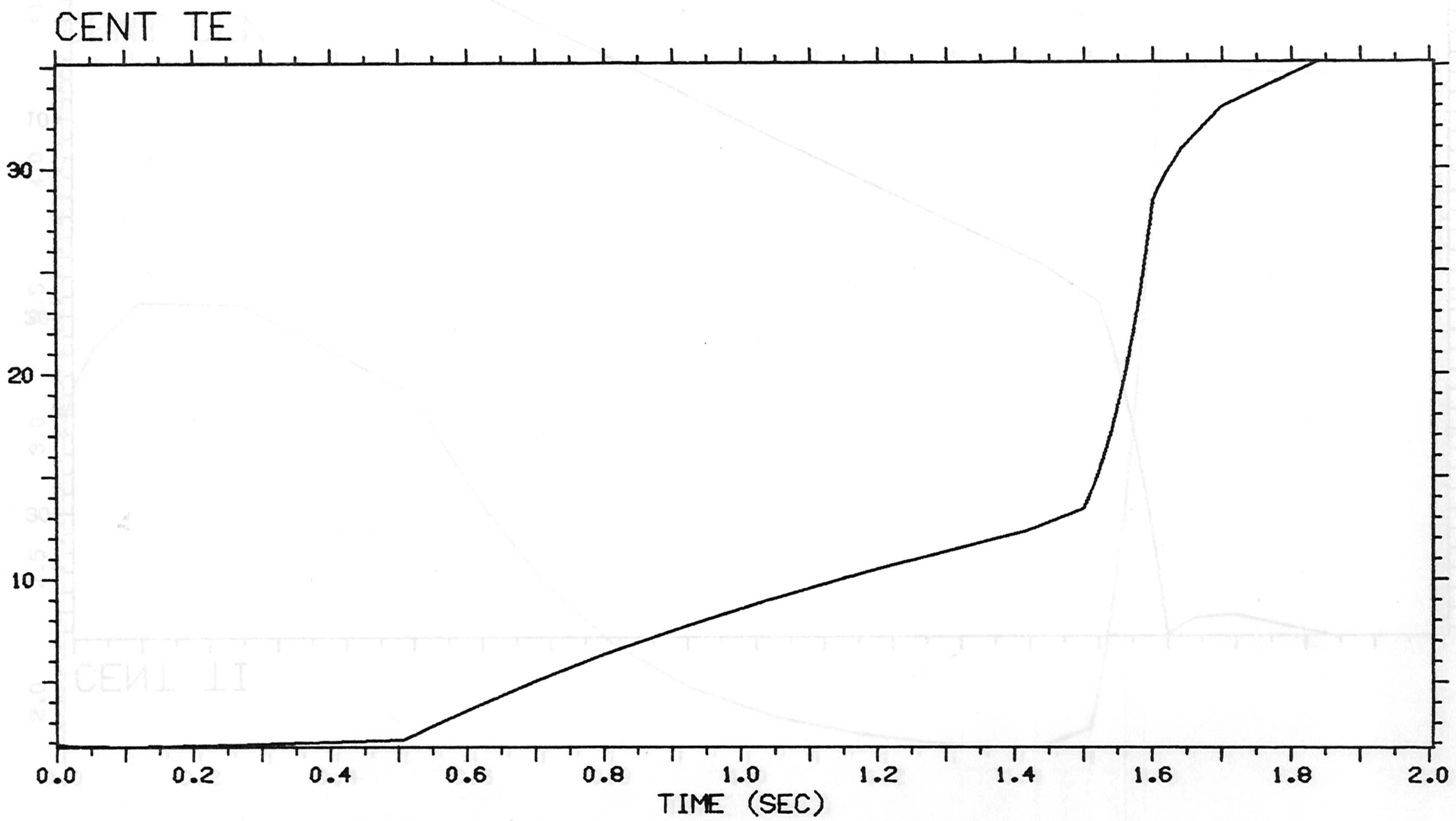

Fig. 3a

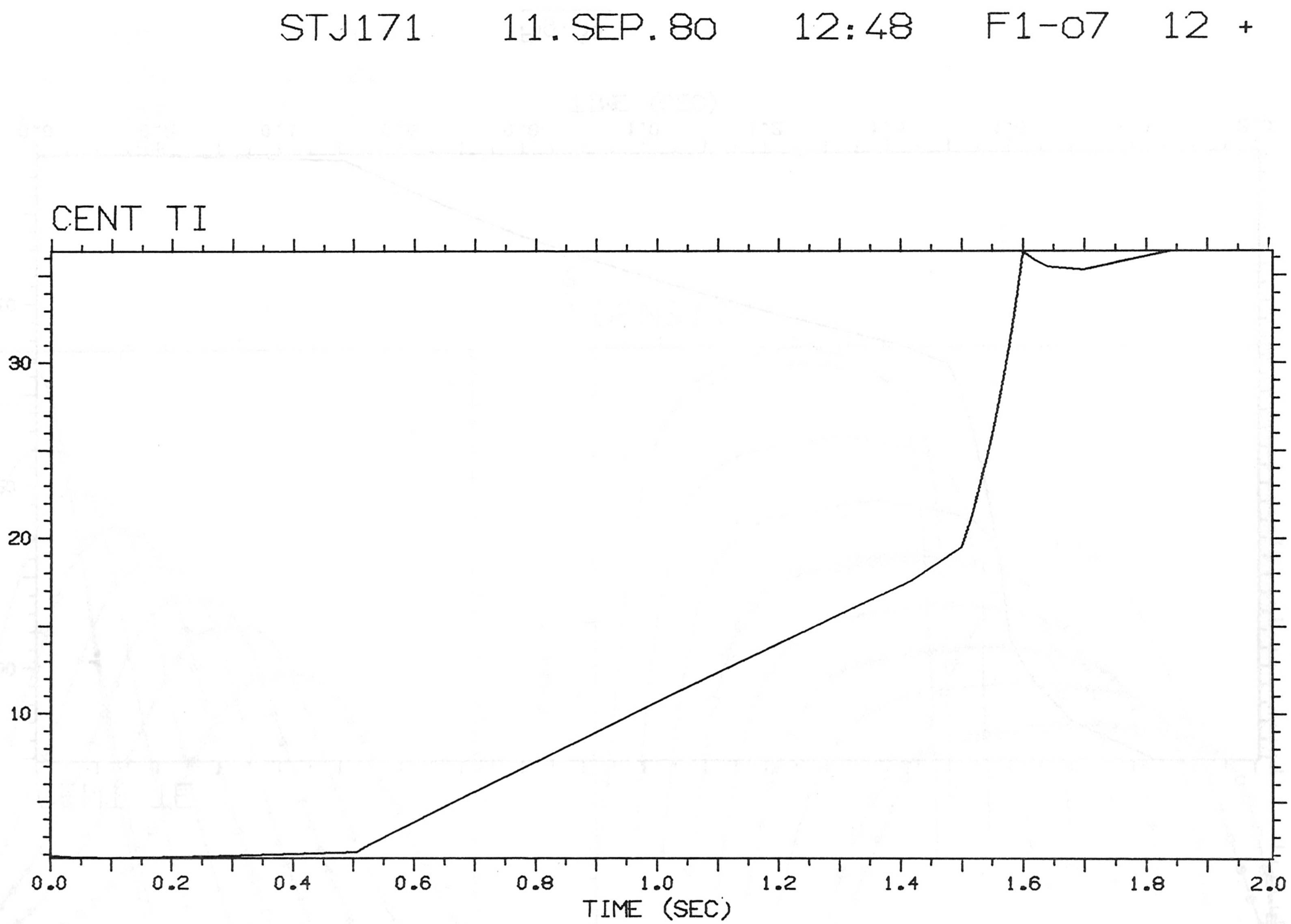
STJ171 11.SEP.80 12:48 F1-07 12 +
CENT TI
30
20
10
0.0
0.2
0.4
0.6
0.8
1.0
1.2
1.4
1.6
1.8
2.0
TIME (SEC)

Fig. 3b

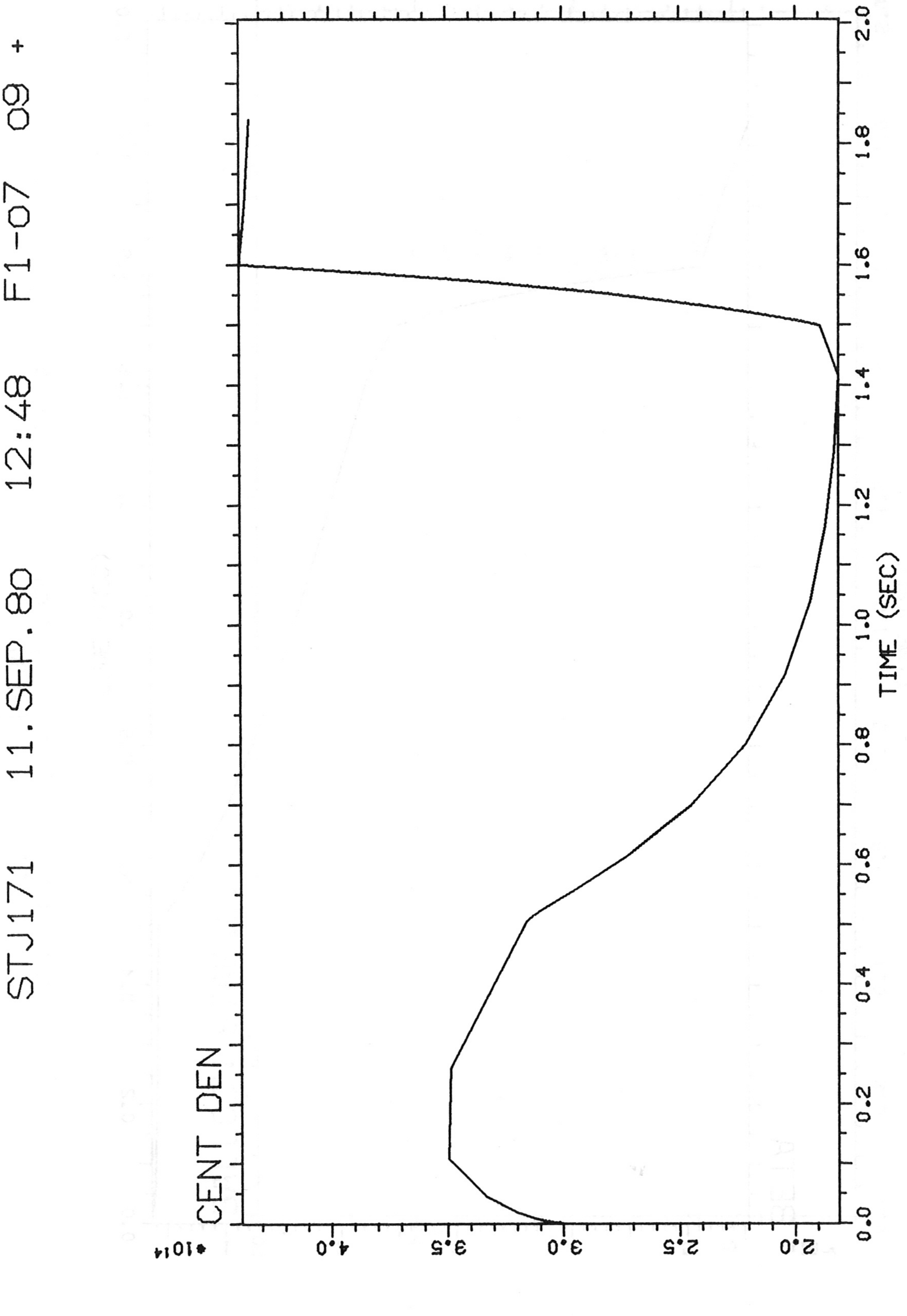
STJ171 11.SEP.80 12:48 F1-07 09 +
CENT DEN
*10¹⁴
2.0
2.5
3.0
3.5
4.0
0.0
0.2
0.4
0.6
0.8
1.0
1.2
1.4
1.6
1.8
2.0
TIME (SEC)

Fig. 3c

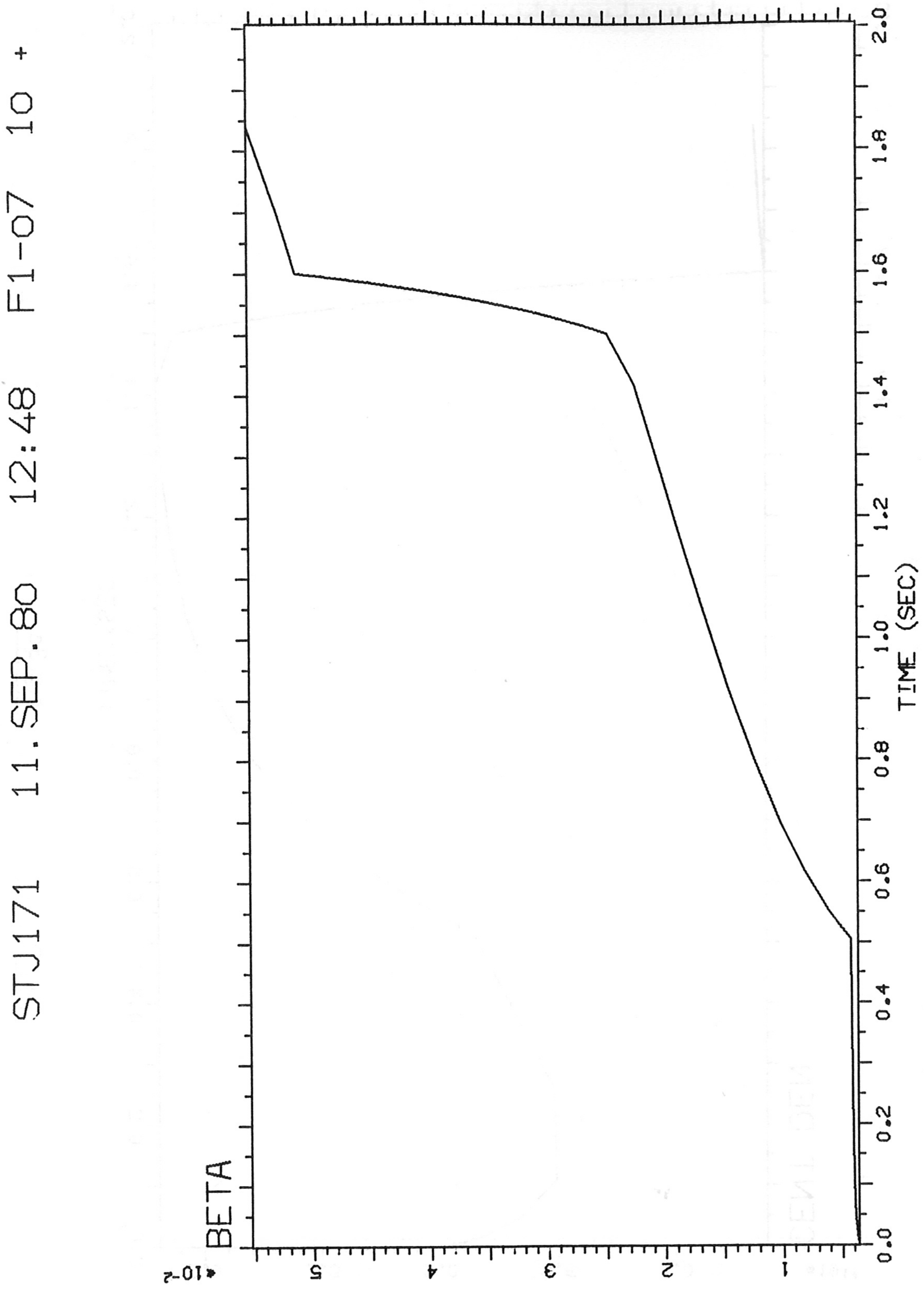

STJ171 11.SEP.80 12:48 F1-07 10 +
BETA
*10-2
5
4
3
2
1
0.0
0.2
0.4
0.6
0.8
1.0
1.2
1.4
1.6
1.8
2.0
TIME (SEC)

Fig.3d

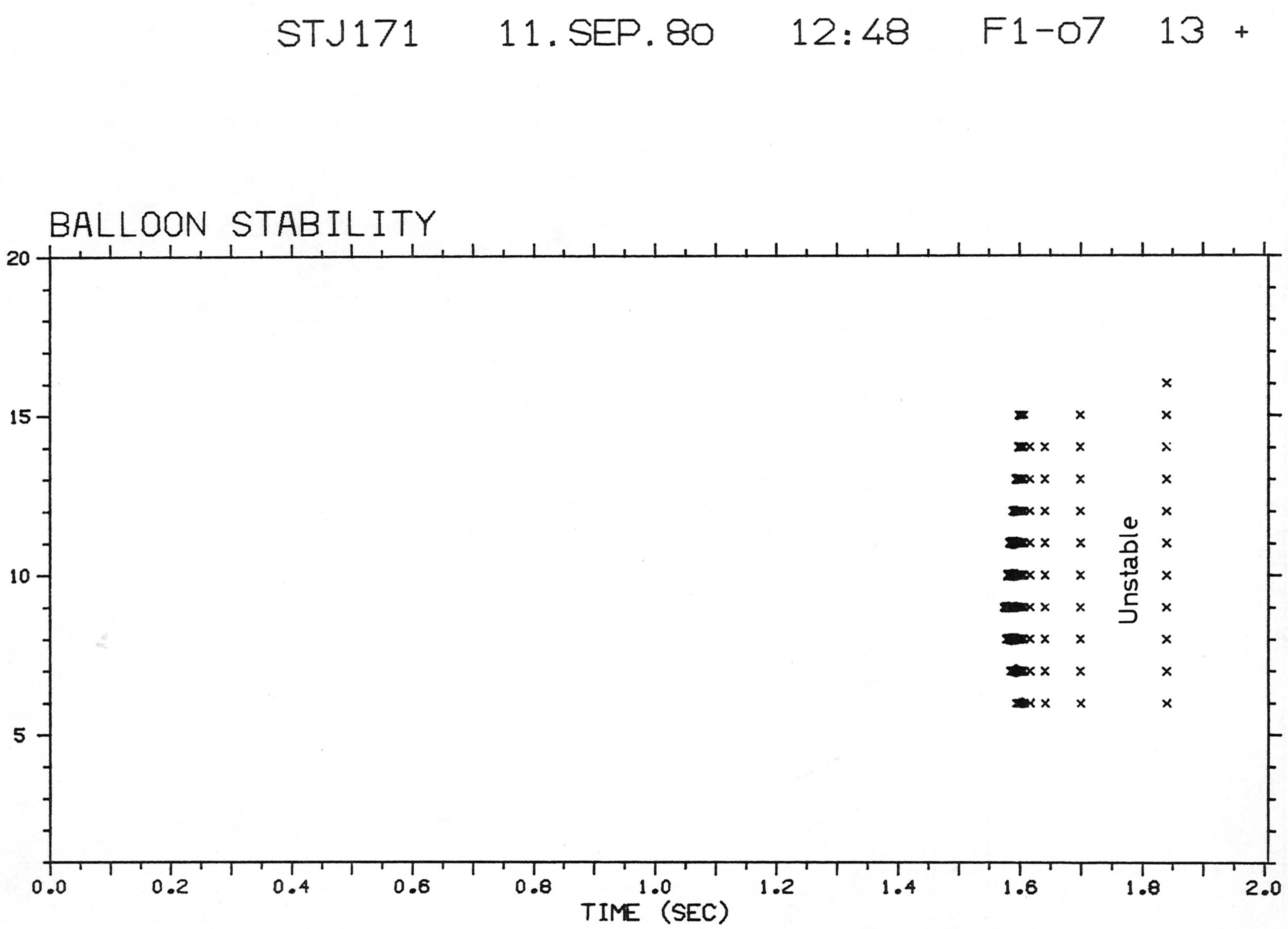
STJ171 11.SEP.80 12:48 F1-07 13 +
BALLOON STABILITY
20
15
10
5
0.0
0.2
0.4
0.6
0.8
1.0
1.2
1.4
1.6
1.8
2.0
TIME (SEC)
Unstable

Figure 4